

<sup>3</sup>C. M. Varma, in *Superconductivity in d- and f-Band Metals*, edited by H. Suhl and M. B. Maple (Academic, New York, 1980).

<sup>4</sup>E. I. Blount and C. M. Varma, *Phys. Rev. Lett.* **42**, 1079 (1979).

<sup>5</sup>H. B. McKay, L. D. Woolf, M. B. Maple, and D. C. Johnson, *Phys. Rev. Lett.* **42**, 918 (1979).

<sup>6</sup>H. R. Ott, W. A. Fertig, D. C. Johnston, M. B. Maple, and B. T. Matthias, *J. Low Temp. Phys.* **33**, 159 (1978).

<sup>7</sup>C. G. Kuper, M. Revzen, and A. Ron, *Phys. Rev. Lett.* **44**, 1545 (1980).

<sup>8</sup>M. Tachiki, A. Kotani, H. Matsumoto, and H. Umezawa, *Solid State Commun.* **31**, 927 (1979).

<sup>9</sup>M. Tachiki, H. Matsumoto, T. Koyama, and H. Umezawa, *Solid State Commun.* **34**, 19 (1980).

<sup>10</sup>The free-energy calculations based on Eq. (2) become inaccurate for  $T \ll T_m$  although the stability range of the various phases is expected to be more or less correct. For  $T=0$ , the free energies of the various phases have been separately calculated. See E. I. Blount, in Proceedings of the Twenty-Sixth Conference on Magnetism and Magnetic Materials, Dallas, Texas, December 1980 (to be published).

<sup>11</sup>C. G. Kuper, M. Revzen, and A. Ron, to be published.

<sup>12</sup>D. E. Moncton, D. B. McWhan, P. H. Schmidt, G. Shirane, W. Thomlinson, M. B. Maple, H. B. McKay, L. D. Woolf, Z. Fisk, and D. C. Johnston, to be published.

<sup>13</sup>J. W. Lynn, G. Shirane, W. Thomlinson, and R. N. Shelton, to be published.

## Resonant Electronic Raman Scattering in Semiconductors

Rainer G. Ulbrich

*Institut für Physik der Universität Dortmund, D-4600 Dortmund, Germany*

and

Nguyen Van Hieu

*Institute for Physics, Nghia Do, Tu Liem, Hanoi, Vietnam*

and

Claude Weisbuch

*Laboratoire de Physique de la Matière Condensée, Ecole Polytechnique, F-91128 Palaiseau, France*

(Received 11 August 1980)

Electronic Raman scattering on shallow donors in semiconductors is enormously enhanced when the incident photon energy approaches the fundamental exciton region. This excitonic resonance was observed for the first time and it was found that  $\sigma_{\text{peak}} \approx 5 \times 10^{-14} \text{ cm}^2$  for CdTe and GaAs in the  $n=2$  free-exciton resonance. The enhancement of  $\approx 10^{10}$  over off-resonance excitation and the peculiar  $n=2$  exciton predominance are well described in a model of exciton-polariton-mediated light scattering.

PACS numbers: 71.36.+c, 71.55.Fr, 78.30.Gt

The inelastic scattering of light by low-lying electronic excitations in solids—electronic Raman scattering (ERS)—has been thoroughly investigated in various configurations since its proposal by Elliott and Loudon.<sup>1</sup> Donor and acceptor excitations in GaP and Si have been studied<sup>2</sup> with fixed incident-light frequencies  $\omega_i$  off resonance, i.e., far below the fundamental band gap  $E_g$ , and extremely small scattering cross sections  $\sigma$  of  $\sim 10^{-25} \text{ cm}^2$  were found. The scattering was described in a *second-order-perturbation* treatment involving interband transitions between one-electron states in valence and conduction bands and reasonable qualitative agreement between theoretical cross sections and experiment was found. Later, Burstein, Pinczuk, and Buchner<sup>3</sup> discussed the relative importance

of *third-order processes* for ERS in the context of resonant light scattering by collective carrier excitations. More recently, Yu studied ERS in relatively highly doped CdS ( $N_D \approx 10^{16} \text{ cm}^{-3}$ ) with  $\omega_i$  below the fundamental exciton.<sup>4</sup> A weak resonant enhancement of  $< 10$  in efficiency was found below the  $I_2$  bound-exciton level and was attributed to resonant interband terms in a perturbation scheme. To our knowledge, the effects of electron-hole correlation and exciton-polariton-mediated resonances on ERS have been neither observed nor discussed up to now.

We report in this Letter the first experimental observation of an enormous resonance enhancement of ERS on shallow donors in semiconductors by a factor of  $\sim 10^{10}$  in  $\sigma$ , when  $\omega_i$  is tuned into the fundamental exciton region. We give an

explanation for the peculiar  $n=2$  free-exciton-mediated resonance which we observed in CdTe and GaAs and we outline a calculation of  $\sigma_{\text{peak}}$  involving effective-mass-donor and *excitonic polariton states* as proper crystal eigenstates for description. The polariton scattering concept, i.e., the correct (nonperturbative) treatment of the long-range  $e-h$  correlation and the exciton-photon interaction,<sup>5,6</sup> is shown to be of fundamental importance for a quantitative explanation of the observed resonant ERS spectra.

The experiments were done at  $T=1.4$  K on cleaved bulk CdTe and as-grown GaAs epitaxial layers oriented in [110] and [100] directions and having neutral shallow donor concentrations  $N_D=(0.8-4)\times 10^{14}$  cm<sup>-3</sup>. The spectra were taken with a 1-m double-grating spectrometer in back-scattering configuration. A cw tunable Oxazine-750 dye laser with  $\leq 0.1$  Å linewidth and  $\sim 5$  mW of incident linearly polarized light power on  $0.2 \times 2$  mm<sup>2</sup> spot size was used for excitation. In the following, we will report for the sake of clarity only the key results in CdTe.

Figure 1 shows highly resolved sections of resonant ERS spectra for six different incident-light energies  $\hbar\omega_i$  around the two dominant resonances which we found: (i) the  $n=2$  exciton  $X_2$  at  $\hbar\omega = 1.6023$  eV (right side), and (ii) the donor-bound exciton  $D^0, X$  at  $\hbar\omega = 1.5927$  eV (left side). The most prominent inelastic ERS peaks are due to the excitation of donor electrons from their 1s ground state into  $n=2$  final states, with a corresponding Stokes shift  $\Delta E_{1s \rightarrow 2s} = 10.62$  meV relative to  $\hbar\omega_i$ , which is indicated by the solid arrows pointing upward in Fig. 1.<sup>7</sup> The enormous increase of scattered-light intensity in very narrow ( $\leq 1$  meV) spectral regions around both the  $X_2$  and the  $D^0, X$  resonances (marked by open arrows pointing downward) is documented in Fig. 1. The ERS peaks were found to be fully polarized; the luminescence background caused by bound-exciton recombination at 1.5899, 1.5912, and 1.5926 eV was unpolarized. In addition to donor  $1s \rightarrow n=2s, 2p$  excitations (with splitting  $\delta E_{2s,2p} = 0.145$  meV<sup>7</sup>) we observed  $n=3$  and  $n=4$  as well as transitions to the continuum (Fig. 1, lower-right and top-left spectrum).

In Fig. 2 we plot the measured scattering efficiencies (defined as the number of outgoing photons per steradian and per incoming photon) for donor  $1s \rightarrow 2s$  and  $1s \rightarrow 2p$  ERS processes as a function of incident photon energy  $\hbar\omega_i$ . The two dominant sharp resonances are centered around the  $X_2$  and the  $D^0, X$  level. The other free-exciton

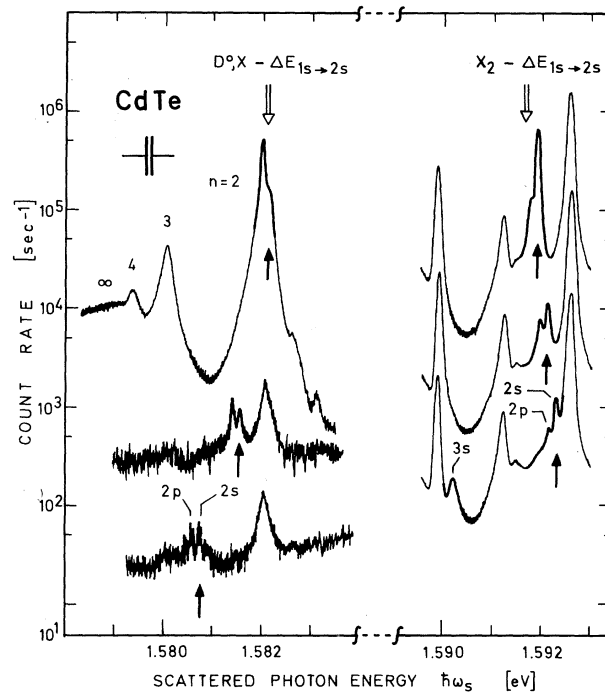


FIG. 1. Resonant ERS spectra of CdTe ( $N_D = 2 \times 10^{14}$  cm<sup>-3</sup>) at  $T=1.4$  K. Spectra for six different incident photon energies  $\hbar\omega_i$  slightly above the  $n=2$  free-exciton resonance  $X_2$  (right side,  $\hbar\omega_i - \hbar\omega_{X_2} = +0.22, +0.43, +0.59$  meV for top, middle, and lower trace) and slightly below the  $D^0, X$  resonance (left side,  $\hbar\omega_i - \hbar\omega_{D^0, X} = -0.0, -0.57, -1.36$  meV) are shown. The solid arrows pointing upward indicate the corresponding six peak positions for scattered photons leaving donor electrons in their excited  $2s$  final state, from which  $\Delta E_{1s \rightarrow 2s}$  was determined. Further scattering channels involving different donor final states ( $2p$  and  $n=3, 4, \dots, \infty$ ) are also indicated. The open arrows pointing downward mark the exact positions of both resonance energies with respect to the  $1s \rightarrow 2s$  process. The lower left and the two lower right traces were each shifted down by a factor of 10 for clarity.

levels  $X_n$  ( $n=1, 3, 4, \dots$ ) do not mediate resonances of comparable strength and narrow width. To compare our results with the off-resonant data of Ref. 2, we used a relative calibration procedure (via LO-phonon Raman signals) and found a ten-orders-of-magnitude resonance enhancement of  $\sigma$  per donor! We will show in the following that one definitely has to go beyond second-order processes and perturbative treatments of ERS to explain this enormous effect.

The usually adopted procedure—iteration of the  $\vec{A} \cdot \vec{p}$  interaction of photons with one-electron states as shown in the second-order diagram of

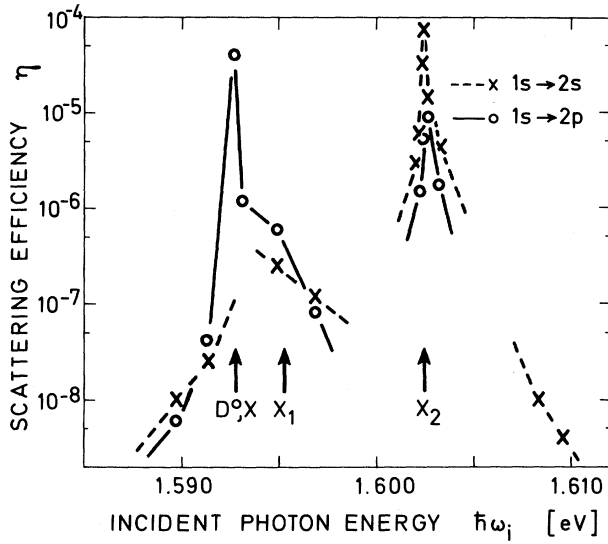


FIG. 2. Experimental electronic Raman scattering efficiency  $\eta$  per steradian for the donor  $1s \rightarrow 2s$  and  $1s \rightarrow 2p$  excitation process as a function of incident photon energy  $\hbar\omega_i$ .  $\eta$  reaches the enormous value of  $8 \times 10^{-5}$  when  $\hbar\omega_i$  is resonant with the  $n=2$  excitonic polariton, other free-exciton levels being less efficient. Lines connect the experimental points for clarity.

Fig. 3(a)—leads under off-resonance conditions to very small cross sections of the order of the classical Thomson value  $\sigma_0 = 6 \times 10^{-25} \text{ cm}^2$ .<sup>1,8</sup> This is in qualitative agreement with the early off-resonant experiments.<sup>2</sup> Within the effective-mass approximation for donors,  $\sigma$  would even vanish because of the orthogonality of the  $n=1$  and  $n=2$  donor levels.<sup>1</sup> Only in the continuum “resonance” region, where  $\hbar\omega_i \geq E_g - E_D$  is fulfilled ( $E_D$  is the donor binding energy), would this procedure lead to relatively large “resonant,” but nondiverging cross sections<sup>9</sup>:

$$\sigma \approx a_B^2 (v_{el}/v_{ph})^2 \approx 10^{-19} \text{ cm}^2, \quad (1)$$

because of the smallness of the energy denominator  $\hbar\omega - (E_g - E_D)$  in the perturbation formula. Here  $a_B$  is the donor Bohr radius,  $v_{ph}$  the photon velocity  $c/n_b$  in the medium of background refractive index  $n_b$ ,  $v_{el}$  the conduction electron velocity at the wave vector  $k = n_b E_g / \hbar c$ .

Our experimental findings—an extremely large  $\sigma_{\text{peak}} \approx 5 \times 10^{-14} \text{ cm}^2$ —clearly show the inadequacy of such a two-step perturbative approach. One has to resort to higher-order processes involving *electron-hole pairs* and take into account their correlation.<sup>10</sup> The new scheme is indicated in Fig. 3(b): The third-order diagram describes the

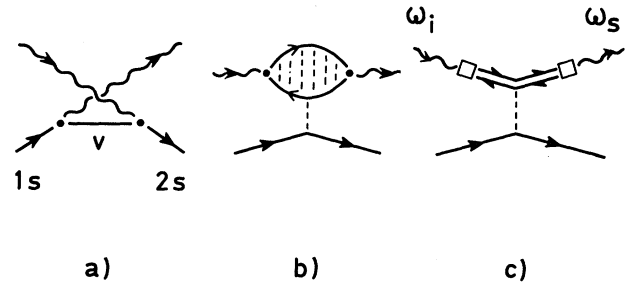


FIG. 3. Electronic Raman-scattering processes: (a) Diagram in second-order perturbation based on the iterated  $\vec{A} \cdot \vec{p}$  interaction term ( $v$  denotes intermediate valence-band states). (b) Exciton-mediated scattering process in third order. Only the direct donor electron-hole interaction term is shown for simplicity (four other terms have to be added; see text). (c) Polariton-mediated scattering. The incident photon  $\omega_i$  converts to a polariton (double line) at the crystal interface, which in turn scatters on the donor electron like the corresponding exciton of (b). The scattered polariton converts back into a scattered photon  $\omega_s$  at the interface.

generation of an  $e-h$  pair by an incident photon, the subsequent interaction of the correlated  $e-h$  pair (“exciton”) via screened Coulomb interaction with the donor-bound electron, and finally conversion of the pair back into a scattered photon. For simplicity, only the direct interaction of the hole with the donor electron is represented. Four other related diagrams (including exchange) have to be considered also for the evaluation of the total scattering probability.

When the exciton-photon interaction is strong (the usual case in the direct-band-gap semiconductors discussed here), it cannot be treated as a perturbation and one has to consider the propagation of coupled-mode excitations in the crystal, i.e., the excitonic polaritons. In the framework of polariton scattering<sup>6,11</sup> the total scattering process may now be visualized to occur in three steps [see the diagram of Fig. 3(c)]: The incident photon converts at the crystal interface into a polariton (with efficiency  $\approx 1$ ), then the polariton is scattered by the donor electron into another polariton state and is finally converted back into a scattered photon (with efficiency  $\approx 1$ ). The total scattering efficiency is almost completely determined by the *polariton-donor interaction strength* alone, which in favorable cases can be treated in first-order perturbation theory.<sup>11</sup>

To test the validity of the latter approach, we calculate the total scattering cross section at the

free-exciton resonance, taking the polariton-donor interaction to be equal to the exciton-donor interaction at the same wave vector<sup>11</sup> and treating it in Born approximation. We find

$$\sigma \approx a_B^2 \mathcal{F}^2 v_{ex}^2 / v_{in} v_{out} \quad (2)$$

where  $v_{ex}$ ,  $v_{in}$ , and  $v_{out}$  are group velocities of the bare exciton, and the ingoing and outgoing polaritons at the polariton wave vector.  $\mathcal{F}$  represents the sum of five dimensionless two-center Coulomb integrals between initial and final states of the scattering process.  $\mathcal{F}$  was calculated numerically and is of the order of unity.<sup>9</sup> Comparing Eq. (2) with the simple perturbative approach of Eq. (1), we gain a factor of  $\sim 10^5$  in our model of polariton-mediated ERS! Using experimentally determined exciton parameters for CdTe {LT splitting 0.4 meV, translational heavy-exciton mass ( $1.3 m_0$ ) along [110], and exciton Bohr radius ( $85 \text{ \AA}$ )}, we find from Eq. (2) an estimate for the maximum cross section  $\sigma_{peak} \approx 10^{-14} \text{ cm}^2$  at the  $X_2$  resonance. The dependence of  $\sigma$  on ingoing and outgoing polariton group velocities explains why the  $X_2$  resonance in Fig. 2 is much more pronounced than the remaining  $X_n$  ( $n = 1, 3, 4, \dots$ ) resonances: The donor  $1s \rightarrow 2s$  energy is close to the  $X_2 \rightarrow X_1$  energy separation and causes a "doubly" resonant behavior of the denominator in Eq. (2).

The theoretical cross sections are converted into an efficiency per steradian,  $\eta$  (ordinate unit of Fig. 2), by calculating

$$\eta = N_D \sigma L / 4\pi, \quad (3)$$

where  $L$  is the effective polariton damping length. Taking  $L$  to be  $10^{-4} \text{ cm}$  (the reciprocal measured absorption coefficient at the peak of  $X_2$ ) we find a theoretical  $\eta_{peak} \approx 1.6 \times 10^{-5}$ . The fair agreement with the experimentally determined peak efficiency of  $8 \times 10^{-5}$  (see Fig. 2) asserts the validity of the proposed model. In addition, Eq. (2) predicts the correct ratio between  $X_1$  and  $X_2$  ERS efficiencies (see Fig. 2) due to the different final states densities. Attempts to treat the sharp  $D^0, X$  resonance along similar lines turn out to be more difficult: (i) Simple perturbative methods (i.e., the first Born approximation for polariton scattering on donors) fail probably in this case of a relatively strong attractive potential with a series of bound states, and (ii)  $D^0, X$  wave functions of sufficient accuracy for ground and excited states are not at hand.

In conclusion, we have demonstrated that the cross section for resonant ERS on shallow donors

in semiconductors is enormously enhanced as a consequence of electron-hole correlation and the excitonic-polariton effect. The analysis of scattering formulas shows that at resonance the three-step scattering probability reduces to a first-order polariton scattering probability. This new approach overcomes the second-order-perturbation results (weak direct iterated  $\vec{A} \cdot \vec{p}$  interaction between localized donor and delocalized one-electron band states) by five orders of magnitude in  $\sigma$  and brings qualitative agreement with experiment. Apart from this conceptual success of the polariton description of resonant light scattering, future applications of resonant ERS will include the possibility of impurity-level spectroscopy with excellent sensitivity in the visible spectral range<sup>7</sup> and with high spatial resolution for the chemical analysis of shallow impurities in semiconductors.

It is a pleasure to thank R. Triboulet (Centre National de la Recherche Scientifique, Bellevue-Meudon) and E. Bauser (Darmstadt; now at Max-Planck-Institut für Festkörperforschung, Stuttgart) for the gift of CdTe and GaAs samples. The participation of A. Nakamura (now at the Institute for Solid State Physics, Tokyo) in the early stage of this work is gratefully acknowledged.

<sup>1</sup>R. J. Elliott and R. Loudon, *Phys. Lett.* **3**, 189 (1963); for a survey, see M. V. Klein, in *Light Scattering in Solids*, edited by M. Cardona (Springer, Berlin, 1975), Chap. 4, and references therein.

<sup>2</sup>C. H. Henry, J. J. Hopfield, and L. C. Luther, *Phys. Rev. Lett.* **17**, 1178 (1966); G. B. Wright and A. Mooradian, *Phys. Rev. Lett.* **18**, 608 (1967); A. Mooradian, *Phys. Rev. Lett.* **20**, 1102 (1968).

<sup>3</sup>E. Burstein, A. Pinczuk, and S. Buchner, in *Proceedings of the Fifteenth International Conference on Physics of Semiconductors*, edited by B. L. H. Wilson (Institute of Physics, Bristol and London, 1979), p. 1231.

<sup>4</sup>P. Y. Yu, *Phys. Rev. B* **20**, 5286 (1979).

<sup>5</sup>In the context of phonon scattering the importance of  $e-h$  correlation for a quantitative description near the fundamental absorption edge of dielectrics has first been pointed out by A. K. Ganguly and J. L. Birman, *Phys. Rev.* **162**, 806 (1967).

<sup>6</sup>D. L. Mills and E. Burstein, *Phys. Rev.* **188**, 1465 (1967).

<sup>7</sup>The donor excitation energy  $\Delta E_{1s \rightarrow 2s}$  and splitting  $\delta E_{2s, 2p}$  which were measured here with great accuracy both constitute a characteristic fingerprint of the chemical donor species present in the sample and are a consequence of central-cell potentials and electron-phonon interactions. For a discussion of  $1s \rightarrow 2p$  infrared-

spectroscopy results in CdTe, see P. E. Simmonds *et al.*, Phys. Status Solidi (b) **64**, 195 (1974).

<sup>8</sup>P. A. Wolff, Phys. Rev. Lett. **16**, 225 (1966).

<sup>9</sup>A detailed treatment of resonant ERS will be given

elsewhere.

<sup>10</sup>R. Loudon, Proc. Roy. Soc. London, Ser. A **275**, 218 (1963).

<sup>11</sup>J. J. Hopfield, Phys. Rev. **182**, 945 (1969).

## Silver-Molecule Separation Dependence of Surface-Enhanced Raman Scattering

C. A. Murray, D. L. Allara, and M. Rhinewine

*Bell Laboratories, Murray Hill, New Jersey 07974*

(Received 4 August 1980)

Surface-enhanced Raman scattering from a layer of organic molecules adsorbed on aluminum oxide and covered by a controlled-roughness silver film has been studied. The molecule-silver distance dependence of the Raman-scattering enhancement by the surface was measured in four separate experiments. Large enhancements ( $\sim 10^3$ ) persist in our samples for molecule-silver separation as large as 100 Å, and thus the use of surface-enhanced Raman scattering is shown to be a viable technique for vibrational spectroscopy of a large variety of interface systems.

PACS numbers: 78.30.Jw, 68.20.+t

The discovery<sup>1</sup> of surface-enhanced Raman scattering (SERS), giant enhancements of the order of  $10^4$ – $10^6$  of the Raman scattering from monolayers of certain molecules on roughened surfaces of silver, has aroused considerable excitement. Numerous models have been proposed to explain SERS,<sup>2-17</sup> but to date, its microscopic origins are still controversial.<sup>2</sup> We report in this Letter the results of SERS experiments which use samples that are thin-film multilayered structures of Al/Al<sub>2</sub>O<sub>3</sub>/Raman-active molecule/spacer/rough Ag film. We find a large ( $\sim 10^3$ ) SERS for molecules

separated by distances  $\sim 100$  Å from the silver surface. This enhancement is adequate for observing a monolayer of molecules of ordinary Raman cross section with present experimental techniques.

We have performed two types of experiments: (a) A smooth layer of a weak Raman scatterer, poly-methylmethacrylate (PMMA), was placed between a strongly Raman-active monolayer of chemisorbed *p*-nitrobenzoic acid (PNBA) and a rough Ag film; and (b) variable-thickness films of a strongly Raman-active polymer, poly(*p*-nitro-

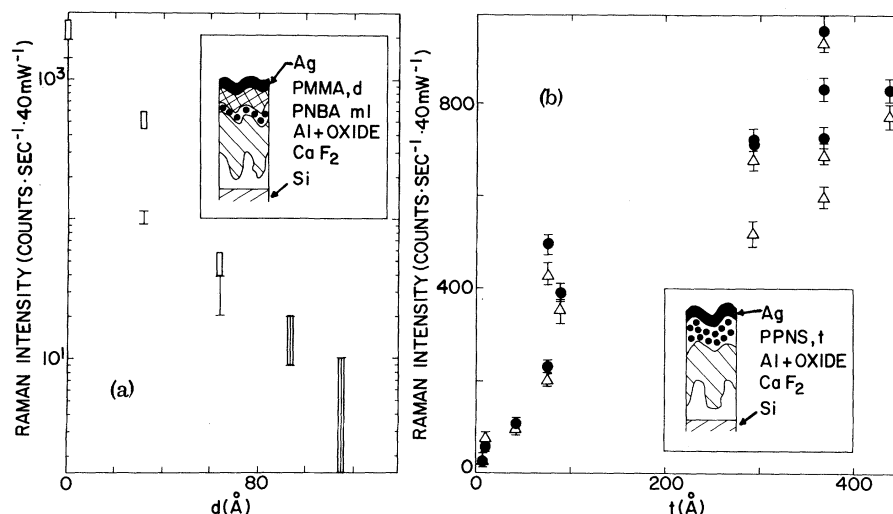


FIG. 1. (a) Spacer experiment 1(a) (inset shows the geometry). The intensity of the 1595-cm<sup>-1</sup> (open symbols) and 1425-cm<sup>-1</sup> (closed symbols) Raman peaks of PNBA above the background (logarithmic scale) vs  $d$ . Error bars are the size of the symbols and represent statistical accuracy only. (b) Thickness experiment 1(b) (inset shows the sample structure). The intensity of the 1596-cm<sup>-1</sup> (circles) and 1346-cm<sup>-1</sup> (triangles) Raman peaks of PPNS above the background (linear scale) vs  $t$ . Error bars represent statistical accuracy only.